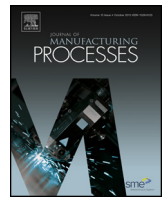




Contents lists available at ScienceDirect

Journal of Manufacturing Processes

journal homepage: [www.elsevier.com/locate/manpro](http://www.elsevier.com/locate/manpro)



## Technical Paper

# Induction heated tool assisted friction-stir welding (i-FSW): A novel hybrid process for joining of thermoplastics

Bandari Vijendra, Abhay Sharma\*

Indian Institute of Technology, Hyderabad, Yeddumailaram 502205, Telangana, India

## ARTICLE INFO

### Article history:

Received 21 February 2015

Received in revised form 4 July 2015

Accepted 6 July 2015

Available online xxx

### Keywords:

Friction-stir welding

Thermoplastics

Induction heating

Tool-pin temperature

Tensile strength

Hardness reduction ratio

## ABSTRACT

This paper presents a hybrid friction-stir welding process, i-FSW, for the joining of thermoplastics. In this process, the friction-stir tool during welding is heated by induction and the temperature is precisely maintained through feedback control. The paper conveys new observations on friction-stir welding of thermoplastics through a case study on the welding of high-density polyethylene plates. The mechanical behavior and weld microstructure were studied over a wide range of tool rotational speeds and tool-pin temperatures. A narrow transition zone between the weld and base materials without any defect ensures joints with a similar strength to the base material, vis-a-vis better than previously reported results with the same material. A drop in hardness at the weld zone, for all the parameters, and a transition from brittle to ductile nature of the joints at higher tool-pin temperatures were observed. The material flow and weld formation mechanism in i-FSW is discussed.

© 2015 The Society of Manufacturing Engineers. Published by Elsevier Ltd. All rights reserved.

## 1. Introduction

The current techniques for welding thick section thermoplastic plates, such as extrusion, hot gas and butt fusion welding, rely on the skill and consistency of the operator to ensure a good weld quality. Recent investigations have shown the capability of the friction-stir welding (FSW) process in potentially replacing the foregoing manual techniques [1]. FSW is a comparatively new welding process that was developed and patented by the welding institute in 1991 [2], initially for aluminum and its alloys. It is a solid-state hot-shear joining process in which a rotating tool with a shoulder and a pin moves along the weld seam as shown in Fig. 1. The frictional heat from the tool shoulder and deformation heat from tool pin enable the material to soften without reaching the melting point. Severe plastic deformation and flow of this plasticized material occurs as the tool is translated along the welding direction. Material is transported from the leading to the trailing edge of the tool, where it is forged to form a joint.

The FSW method may offer many advantages over existing fabrication techniques, such as increased productivity and quality due to ease of automation and possibility of long continuous welds, with an ability to weld almost all thermoplastics [4]. In spite of the potential advantages, the FSW process at present is primarily proved for

producing linear welds. The FSW of plastics is different from that of metals [5], because of differences in material structure and morphology. Unlike metallic materials, polymers have a low-thermal conductivity, low-melting temperature, low hardness, relatively poor impact resistance, and short solidification time. The tool in FSW of some hard metals sometimes need to be externally cooled, whereas the same needs to be externally heated in case of thermoplastics in order to avoid problems with conventional tools, such as squeezing of the polymer from the weld nugget. Researchers have developed a modified tool [6], with a stationary shoulder called a shoe that is heated by electric resistance.

In the recent past, the use of FSW has been reported for variety of thermoplastics. Jaiganesh et al. [7] presented the optimization of process parameters on friction-stir welding of high-density polypropylene plate. Pirizadeh et al. [8] reported a new tool design with two shoulders, known as a self-reacting tool, for mitigating root defects in the FSW of acrylonitrile butadiene styrene (ABS). Mendes et al. [9] examined the factors affecting the FSW of ABS performed by a robotic system using a tool with a stationary shoulder and external heating. Without external heating, the FSW of ABS resulted in maximum joint efficiencies of above 60%, Mendes et al. [10]. Panneerselvam and Lenin [11] observed that in the FSW of Nylon-6, a joint fabricated with counter-clockwise directed tool rotation produced better material properties. Hoseinlghab et al. [12] investigated creep properties of FSW-welded polyethylene plate joints and reported that under controlled conditions, the creep resistance of welds may be better than that of the base

\* Corresponding author. Tel.: +91 4023016091.  
E-mail address: [abhay@iith.ac.in](mailto:abhay@iith.ac.in) (A. Sharma).

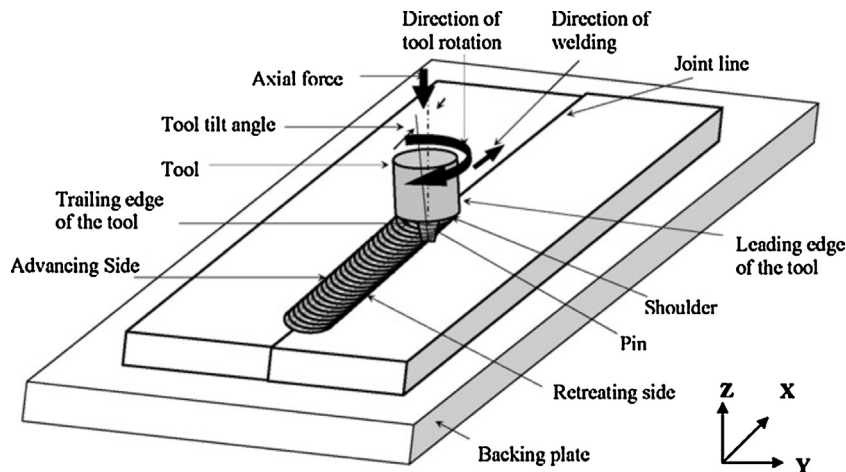


Fig. 1. Schematic of friction-stir welding process [3].

material. Azarsa et al. [13] investigated flexural behavior of high-density polyethylene welds produced with a stationary shoulder (shoe) and a heating system inside the shoe. Bagheri et al. [14] presented FSW of ABS using a fixed heated shoe called a hot shoe, wherein a rotating pin passing through this shoe stirs melted material. Sadeghian et al. [15] reported FSW of ABS with weld strength up to 97 and 101%, respectively for cylindrical and conical pinned tools. Polyethylene plates joined by a conventional FSW tool with an integrated pin and shoulder presented a joint strength of 75% of the base material under optimum welding conditions [16]. The effect of double passes of the tool [17] in the FSW of medium-density polyethylene eliminated the root defect but the joint strength was less than 90% of the base material. Mostafapour and Azarsa [18] reported a joint efficiency of 97% with a shoe-heating method. The effect of preheating on the FSW of ultrahigh molecular weight polyethylene [19] was investigated where the additional heat enabled the material to be easily stirred; and 89% joint efficiency was achieved. Such investigations have limited success because it is difficult to attain a stable tool temperature over a longer weld span. Furthermore, the FSW of polymers is very sensitive to changes in temperature.

The objective of this paper is to demonstrate a new technique of friction-stir welding (i-FSW) of thermoplastics that can overcome the limitations of existing methods, e.g., shoe heating method may not be best for curvilinear welds, pre-heating of tool may not perform lengthier welds because of dip in tool temperature, and external heating of tool may lead to unnecessary heating of base material. The moot point is, if the conventional FSW, which is capable of curvilinear welding, can be modified such that the tool temperature can be maintained over the entire length of the weld. This paper presents such an attempt wherein the FSW tool is induction-heated and precise temperature control is achieved through temperature feedback. The investigation also seeks to assess the efficacy of the proposed process through examination of joint efficiency, weld microstructure, type of fracture, and weld hardness so that a better insight of the FSW of thermoplastics may be developed.

## 2. Experimental procedure

### 2.1. Experimental set up

The i-FSW consists of an induction coil that encircles the FSW tool as shown in Fig. 2a. The induction coil, along with the induction power source, and optical infrared temperature sensor, are mounted on the machine head and move with the tool as shown

in Fig. 2b. When an alternating electrical current is applied to the induction coil, electric eddy currents are induced in the FSW tool that consequently heat it.

The temperature sensor senses the temperature at the tip of the tool and sends signal to the temperature controller, which is synchronized with the induction power source. Once the processing parameters are set, the two pieces to be joined are held tightly in the fixture, ensuring that the parallelism of the sides to be welded is not lost. The tool is heated by induction and once the pin reaches the required temperature, the rotating tool is plunged into the sheets. A dwell time is allowed to let the tool warm up the material by friction and heated tool and then it traverses along the weld line. The heating of the tool by induction is continued throughout the weld line. Once the tool reaches the end of the butt line, it is lifted up together with the induction coil and then heating of the tool is stopped. This arrangement is totally opposite to FSW tool used for metal, alloys, and composites wherein the tool is externally cooled to prevent wearing out of pin, especially in case of hard material like steels. Metal and alloy may be welded with different tool profiles like cylindrical, cylindrical threaded, triangular, tapered-threaded, etc. However, the material flow in thermoplastics can be managed invariably with taper-threaded pin that restricts upward motion of the material. The heated tool helps in plasticizing the material. The tool heat should be sufficient to the extent that the material remains viscous enough to be stirred. Therefore, the tool temperatures need to be set within a very narrow range as described next.

Commercial 5 mm thick high-density polyethylene (HDPE) plates were cut into 170 × 85 mm size sheets for FSW. The properties of the base material as presented in Table 1. The tool used was made of H13 tool steel material with a hardness of 53HRC. The shoulder had a diameter of 10 mm and the pin was taper-threaded with a major and minor diameter of 6 and 5 mm, respectively. The pin length was 3.83 mm. The direction of tool rotation was anti-clockwise to promote a downward flow of material, since the pin was right hand threaded.

The input parameters were chosen through pilot experiments conducted on bead-on-plate (BOP) welds. The amount of flash and visual quality of BOP welds were observed. BOP welds were performed at 1000, 2000, and 3000 rpm, at tool-pin temperature up to 80 °C and tool travels speed at 50 and 100 mm/min. It was observed that, at higher traverse speed material mixing was not proper and small slots were formed or solid HDPE particles were deposited on seam. Temperature higher than 55 °C resulted in heavy flash with light yellow color, which marked onset of burning. Thus, rotational speeds of 1000, 2000, and 3000 rpm and tool-pin temperatures varying from room temperature (case of no tool heating)

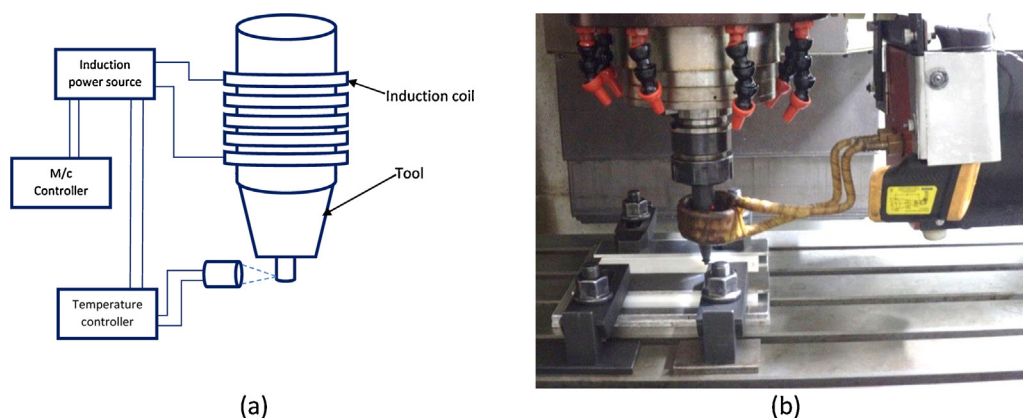


Fig. 2. i-FSW: (a) schematic (b) experimental set-up

**Table 1**  
Properties of HDPE.

Youngs modulus	Yield strength	Density (g/cm <sup>3</sup> )	Melting point (°C)	Hardness	Crystallinity (%)
0.714 Gpa	19.92 Mpa	0.9705	144.4	4.85 HV	36.39

to 55 °C at an interval of 5 °C were chosen as the process parameters for performing butt joints, keeping the traverse speed constant at 50 mm/min.

In the initial step of the welding process, a dwell time of 15 s was allowed to the tool to form a small pool of molten material and then it was traversed along the butt line to form a joint. After welding, the welds were allowed to cool in the fixture for about 15 min to avoid bending caused due to shrinkage of material in the weld zone. Tensile test samples were extracted from each welded joint and tests were carried out according to the ASTM D-638 standard, on a universal testing machine at a crosshead speed of 5 mm/min, without removing the flash. The Vickers hardness test was conducted on the cross section of the welded samples, at distances 1.2 and 2.4 mm above the base. Microstructure examination of the welds was carried out with an optical microscope. Differential scanning calorimetry (DSC) and fourier transform infrared spectroscopy (FTIR) of base material selected welded samples were conducted to understand structural and chemical changes, respectively.

### 3. Results and discussion

#### 3.1. Material flow and tensile strength

The material flow, i.e., ‘flash’, can be controlled by selecting the proper process parameters. Fig. 3 shows four representative cases of flash, namely no flash Fig. 3a, moderate flash Fig. 3b, heavy flash Fig. 3c, and very heavy flash Fig. 3d. It can be seen that changes in rotational speed and temperature greatly influence flash generation. For a change in temperature of 15 °C for same rotation speed, no flash to very heavy flash condition may be obtained, as shown in Fig. 3a and d, respectively. Similarly, change in rotation speed at constant temperature brings a considerable change in flash generation. The visual appearance of welds is important from an esthetic point of view; however, it is not always decisive in terms of joint strength. Fig. 4 shows the effect of rotational speed and tool temperature on joint strength. It can be inferred that when the rotational speed increased from 1000 to 2000 rpm at various temperatures the tensile strength also increased; however, a further increase in rpm caused strength to decrease. Similarly, an increase in temperature from 40 to 45 °C resulted in an increase in strength; however, further increase in temperature caused the strength to decrease at higher tool rotation speed of 3000 rpm.

Though 1000 rpm and tool-pin temperature 40 °C resulted in minimum flash, this combination also resulted in minimum strength. At low rotational speed combined with low tool tip temperature the heat is insufficient and the polymer does not soften enough, resulting in improper fusion between the seam and the base material, as shown in Fig. 5. Stagnant material near the bottom of the seam on the retreating side of the joint indicates improper merging between the weld seam and the adjacent material. The process parameters (i.e., rpm and tool-pin temperature) interactively affect the strength. Increase in rpm is expected to increase temperature and reduce viscosity. However, higher rpm results in heavy flash that weakens the weld by reducing its cross-section area. Thus, a moderate rpm and temperature work optimal for i-FSW in terms of ultimate tensile strength. At the high rotational speed of 3000 rpm, the deformation and frictional heat caused excessive turbulence of material in the seam and hence the flow of softened material could not be controlled. As a result, the strength is reduced compared to that at 2000 rpm where sufficient heat is generated at all the tool-pin temperatures to soften the seam and properly fuse with the base material.

Table 2 shows the joint strength, fracture location, and % elongation. A different set of parameters showed joint strength of about 98.5% or more of the base material and a distinct case of an efficiency

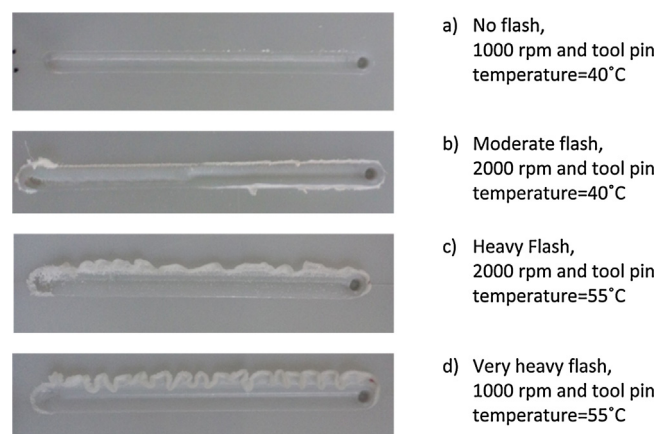


Fig. 3. Flash in samples welded at different parameters



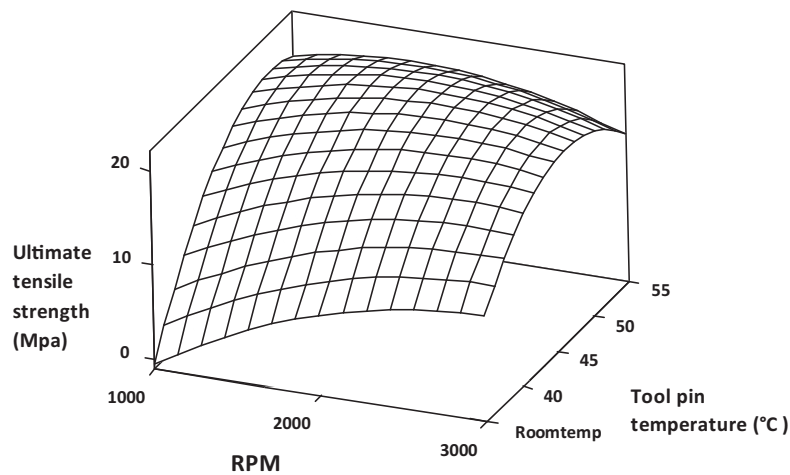


Fig. 4. Effect of tool rotational speed and temperature on tensile strength.

of 104.32% of the base material was found for the weld performed at 2000 rpm and tool-pin temperature of 45 °C. The welded samples fractured at different locations, namely outside the weld seam, at the retreating interface, in the retreating side of the weld seam, at the center of the weld seam, and in the advancing side of the weld seam. The sample that showed the maximum joint efficiency fractured from base material (type a fracture). When the crack formed at the interface of the weld seam and base material in the retreating side (type b) or at the center of the weld (type d) the joint efficiency was between 78–98%. The samples welded at low rpm primarily fractured in the retreating side of the weld bead (type c) and displayed minimum joint efficiency (up to 40%) and minimum elongation as well.

The fracture location and pattern are greatly influenced by shearing or flow developed by the outer perimeter of the tool. Fig. 6 shows transition zone observed at the bottom of the tool pin in retreating side, between the seam and the base material. These welds broke in retreating side during tensile test. The width of the transition zone in case (a) is narrower compared to others. The case (a) represents the weld that was performed at 2000 rpm and a tool-pin temperature of 45 °C; and resulted in the maximum joint efficiency. This is in agreement with the findings of Kiss and Czigany, 2012, who observed that the strength of the FSW joint was close to that of the base material if the overall width of the transition zone is small and the less complex its morphology. The width of the transition zone is controlled by cooling, molecular alignment/relaxation, and crystallization, where crystallization plays the most important role. A wider zone can be observed in

the case of the weld that was performed at 1000 rpm and a tool-pin temperature of 50 °C, as shown in Fig. 6b. In this case, fracture occurred in the weld material and the joint efficiency was quite low. In the absence of sufficient rotational speed, even if the temperature was increased to 50 °C, proper fusion between weld material and base material was not obtained. A crack, at the weld and base material interface, can be observed in Fig. 6b. When the rotation speed was increased to 3000 rpm, the transition zone was uniform but wider and more clearly visible (Fig. 6c) than the maximum joint efficiency condition of 2000 rpm (Fig. 6a).

The transition zone is due to skin-core structure formation in weld. The central part of weld seam (core) cools slowly, while more intense heat withdrawal occurs at base material and weld interface (i.e., skin). Thus, spherulitic crystallization could take place in core section, while supermolecular structure is formed in the skin. Moreover, temperature generated due to pin rotation in FSW helps in crystallization because of longer molecular relaxation time [20]. As a result, narrow transition zone width is obtained at higher temperature. The skin-core postulation is verified with help of DSC. Fig. 7 gives a typical DSC results obtained for a sample taken from the weld seam and base material.

The transition zone formation is directly related with heat distribution pattern and morphology of thermoplastic welds. The existence of a wider transition zone indicates a larger extent of change in structure of the material, e.g., the sample obtained at 1000 rpm that exhibited wider transition zone showed crystallinity drastically reduced to 13%. However, the samples welded at higher tool rotation speed such as 2000 rpm showed 34% crystallinity, which was close to base material (i.e., 36%). With increase in rpm to 3000 crystallinity increased to 39%. The transition zone formation also reflects on the chemical changes in the welds as obtained with FTIR. Samples with narrow transition zone exhibited chemical similarity with the base material. Fig. 8 gives IR spectra of base material and welds obtained at higher, moderate, and lower heat input represented by 3000 rpm and 50 °C, 2000 rpm and 45 °C, and 1000 rpm and 40 °C, respectively. The IR spectra of weld obtained at higher heat input (i.e., 3000 rpm and 50 °C) resembles more with base material as shown in Fig. 8. In these two cases, similar bands (i.e., strong bands at 2912 and 2845  $\text{cm}^{-1}$ , which is due to the asymmetric and symmetric stretching frequency of C–H group, a medium band at about 1465  $\text{cm}^{-1}$  due to stretching frequency of the C–C bond and medium band at 721  $\text{cm}^{-1}$ ) are observed, which are not observed at moderate and lower heat input welds. The IR spectra of weld at 2000 rpm and 45 °C showed a strong band (close to 800  $\text{cm}^{-1}$ ) similar to that observed with weld produced at 3000 rpm and 50°. This band indicates presence of the aromatic functional



Fig. 5. Stagnant solid material near the bottom of the seam at the retreating side of the joint at 1000 rpm and tool-pin temperature 40 °C.

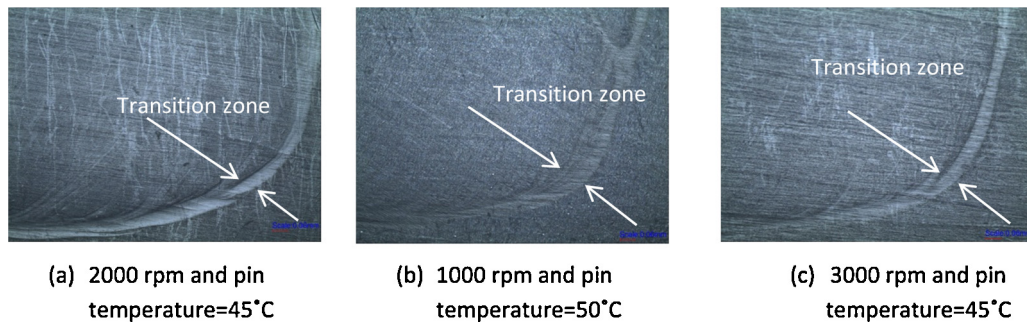


Fig. 6. Transition zone at different welding conditions.

group and signifies the chemical change i-FSW brings at moderate and high heat input. In case of 2000 rpm weak bands in range of  $1665\text{--}1760\text{ cm}^{-1}$  are observed that is related with oxidation. The oxidation range becomes stronger with low heat input weld. Moreover, phenomenon of chain breaking (observed at bands of 900, 1177, 1368, 1375, and  $1678\text{ cm}^{-1}$ ) is observed. Thus, it can be said that higher relaxation time due to high heat input helps in preserving internal structure of welds; however, flash formation lowers strength a bit as described in the initial part of this section.

### 3.2. Stress–strain curves and their relation with fracture locations

The fracture locations and stress–strain curves obtained for low tool temperature welds, as shown in Fig. 9, indicate that all the joints failed in a brittle manner where there was a sudden drop in the strength after reaching the ultimate tensile strength Fig. 11.

The strength of the joints was reduced in all the parameters at a tool-pin temperature of  $50^\circ\text{C}$ , shown in Fig. 12 compared to Fig. 10, since this temperature marks the onset of flash at the retreating side

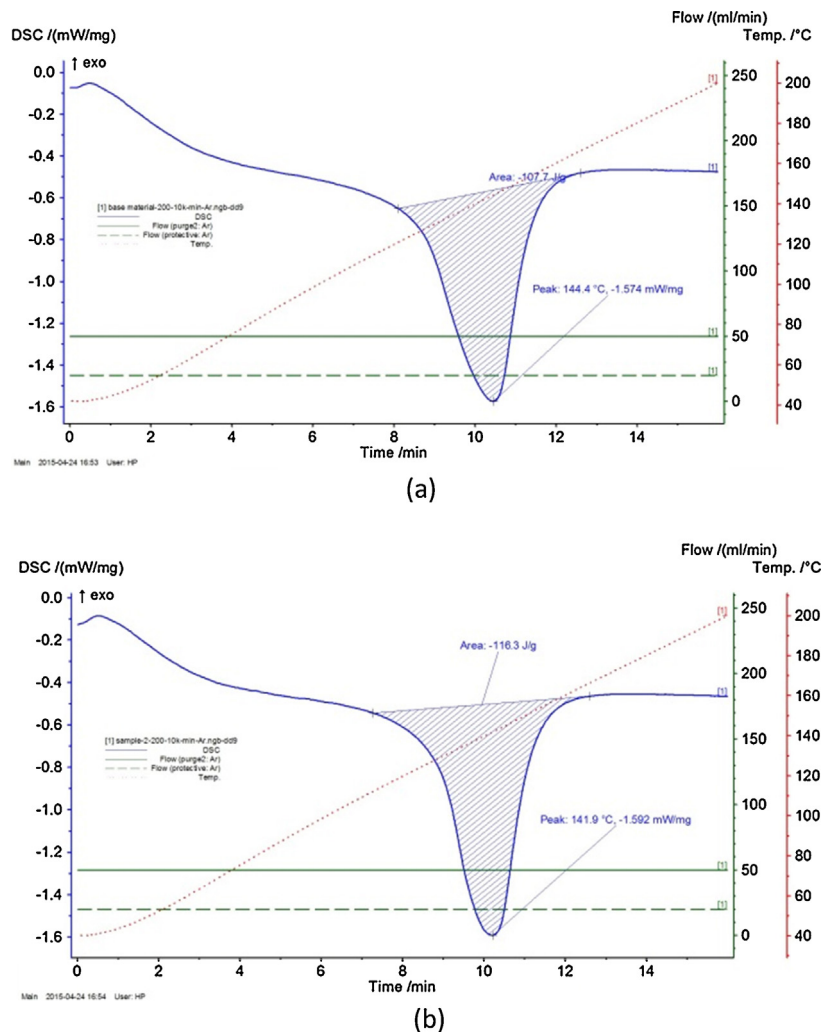


Fig. 7. DSC results of: (a) base material and (b) welded sample.

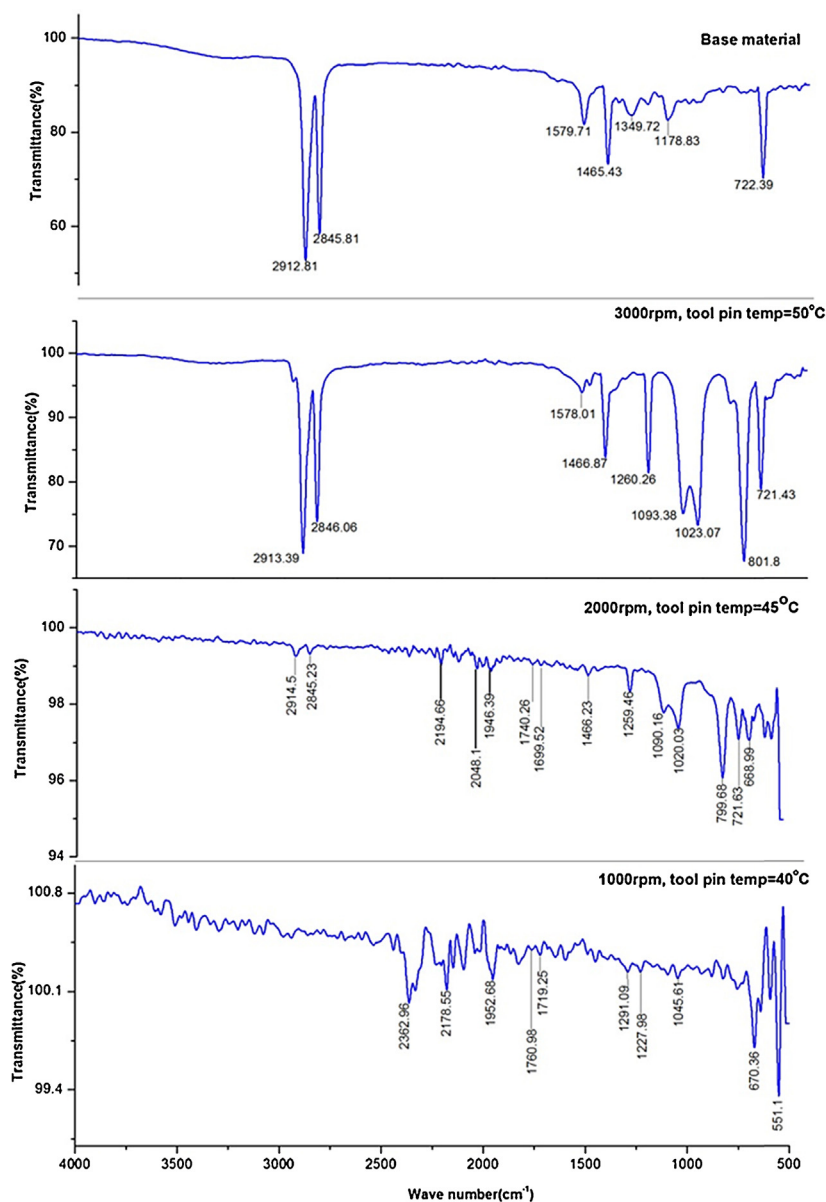


Fig. 8. FTIR results of base material and welded samples.

of the welds that reduced the strength, whereas in the former case material retention within the seam contributed to an increase in joint strength. There is a sudden reduction in strength after reaching the optimum strength in all joints in Fig. 10, which is not the case in Fig. 12, indicating that the strength is governed by the ductility of the joints. At a tool-pin temperature of 55 °C the elongation (in percentage) of all the joints increased as shown in Fig. 13 compared to with Fig. 12 and a fibrous structure was seen at the fracture locations. Compared with a tool-pin temperature of 50 °C, joint strength increased at 55 °C for cases of 1000 and 2000 rpm, along with an increase in flash. The reason being that width of transition zone between seam and the base was narrow that governed strength of the joints, as discussed earlier. In all the four Figs. 9, 10, 12, 13, the welds performed at 2000 rpm, were well above the remaining curves indicating that this rpm had a strong effect on the mechanical properties (i.e., joint strength).

The mechanism of material flow and weld formation is quite different in polymers compared to metals. Initially, when the tool pin comes in contact with the work piece, plasticized material is

formed, which is surrounded by the bottom of the shoulder, cooler base material adjacent to the pin and the backing plate at the bottom. When linear motion is given to the tool, material from the leading edge is progressively plasticized and flows from the retreating side to the advancing side and vice versa. During this transfer, if the resistance to the flow of the plasticized material between the tool and the base material is high, material will flow out of the weld cavity, which mainly happens on the retreating side, since the peripheral velocity of the tool is opposite to the traverse direction. At the advancing side material coming from the retreating side is extruded against the side wall base material where the pressure generated by the flow of material is sufficient to consolidate it giving rise to an almost continuous joint interface as shown in Fig. 14. The zone I indicates retreating side deformation zone and II indicates advancing side deformation zone.

In i-FSW, at high tool-pin temperatures, the shoulder driven material is squeezed out rather than entering into zone II, which happens in the case of metals [21] and it is mainly the pin-driven flow volume that contributes to joint formation. In metals, the

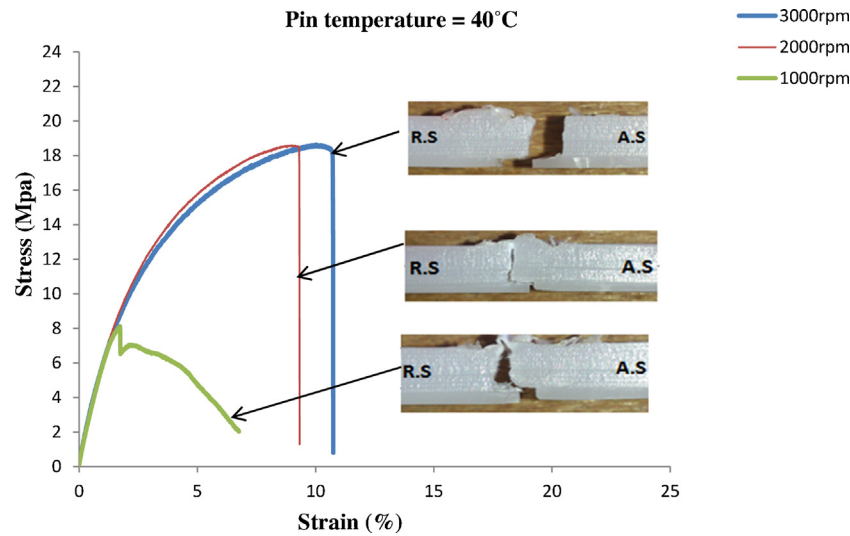


**Fig. 9.** Stress–strain curves and fracture locations at tool-pin temperature of 40 °C.

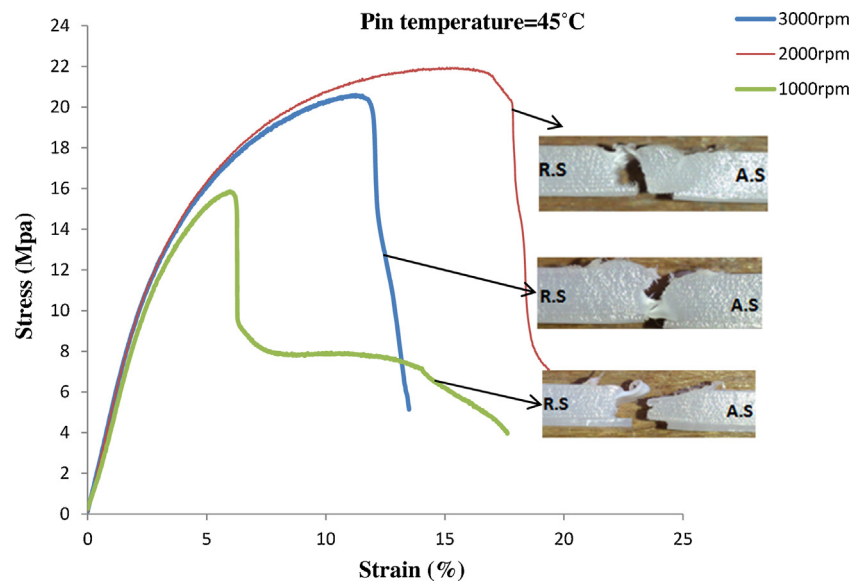


**Fig. 10.** Stress–strain curves and fracture locations at tool-pin temperature of 45 °C.

welds result from the coalescence of the shoulder and pin-driven material flow; that happens at low tool-pin temperatures in the case of i-FSW. At the advancing side, where the peripheral velocity of the pin and traverse of the tool have the same direction, a

polymer element spends a longer time and is more influenced by the velocity field. Hence, the grain structure is more refined and the resultant hardening is higher than on the retreating side. This is discussed in detail in the following section.

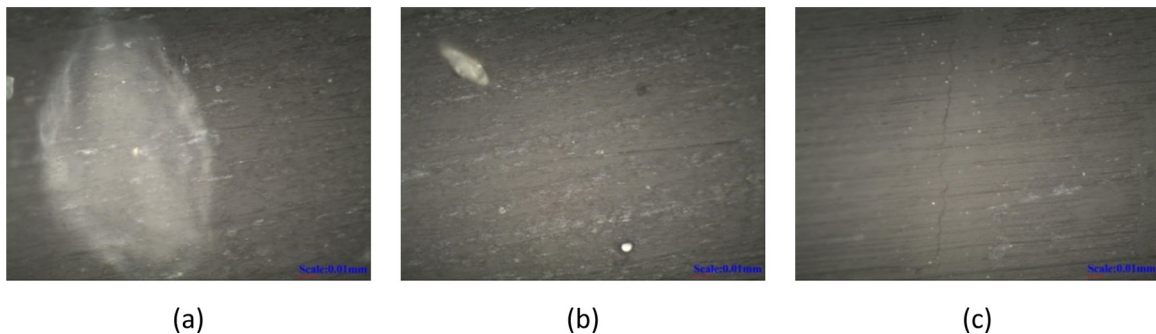


**Fig. 11.** Defects in the weld joint made at 3000 rpm and tool-pin temperature of 45 °C: (a) top region, large pore, (b) middle region, small pores, (c) bottom region, appearance of crack.



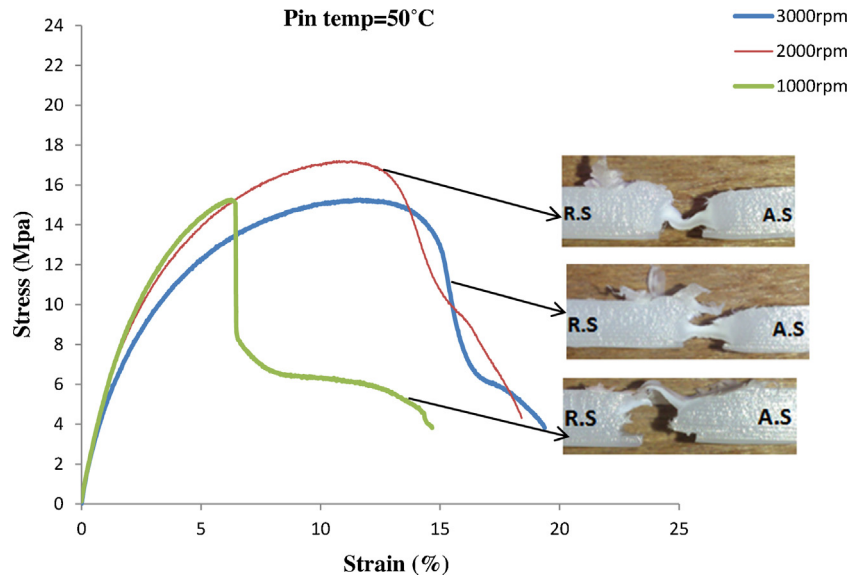


Fig. 12. Stress–strain curves and fracture locations at tool-pin temperature of 50 °C.

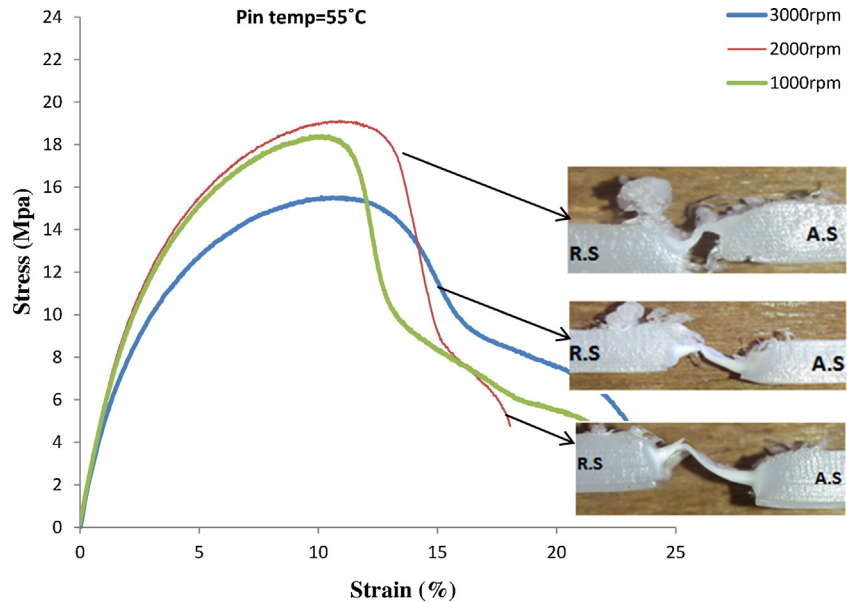


Fig. 13. Stress–strain curves and fracture locations at tool-pin temperature of 55 °C.

### 3.3. Hardness results

Micro Vickers hardness was measured at an applied load of 100 g with a dwell time of 15 s at 2.4 mm above the bottom of the specimen. Figs. 15–17 shows the hardness distribution at the cross section of the joints welded with different process parameters. The weld zone (–5 to +5 mm) showed lower hardness value compared

to the base material. The drop in hardness is due to softening of material caused by the heated tool. From Figs. 13–15, the drop in hardness at the stir zone or pin influence zone, which is approximately –2 to +2 mm from the center of the seam, is greater at a tool-pin temperature of 55 °C compared with that at 40 °C, showing a decrease in hardness with increase in temperature.

The observed hardness pattern is mainly due to the ductile nature of the joints, as evidenced from the fracture locations. Hardness reduction ratio at the weld center [22], as shown in Eq. (1), is a good indicator in understanding the behavior of the weld joint.

Hardness reduction ratio at weld center(%)

$$= \frac{(\text{Basematerial, HV} - \text{Weldcenter, HV})}{\text{Basematerial, HV}} \quad (1)$$

Comparing Figs. 18 and 19, the hardness reduction ratio showed the same tendency with the joint efficiency; that is with a decrease in the hardness reduction ratio the joint efficiency increased at



Fig. 14. Representation of deformation zones in the transverse section of a tensile-tested sample.



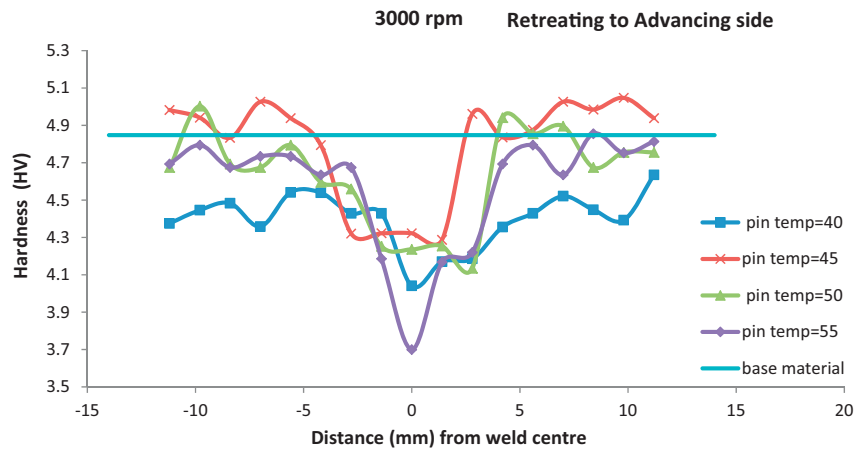


Fig. 15. Hardness plot at 3000 rpm and different tool-pin temperatures.

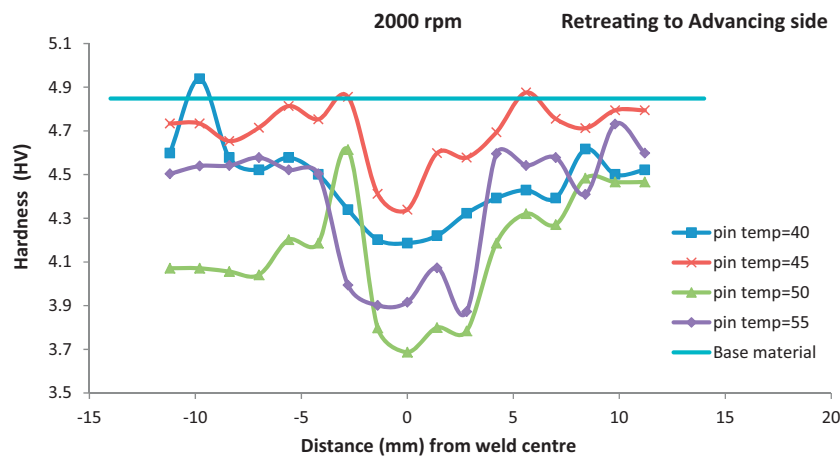


Fig. 16. Hardness plot at 2000 rpm and different tool-pin temperatures.

tool-pin temperatures of 40 and 45 °C. This effect was not seen at higher tool-pin temperatures of 50 and 55 °C for the cases of 1000 and 2000 rpm. At these temperatures, fibers were observed at the fracture locations and the strength was mainly governed by the ductility of the joints. The joint produced at 1000 rpm and 40 °C was an exception, since in this case the fusion of seam and base material at the retreating side was improper (shown in Fig. 5) and

the joint failed in a brittle manner. The minimum hardness reduction ratio, other than the above mentioned case was seen for the weld performed at 2000 rpm and a tool-pin temperature of 45 °C, which showed the highest value of joint efficiency among other welds, also shown in Fig. 19.

It is evident from Fig. 17, that joint efficiency for the welds performed at room temperature (without tool heating) is quite low

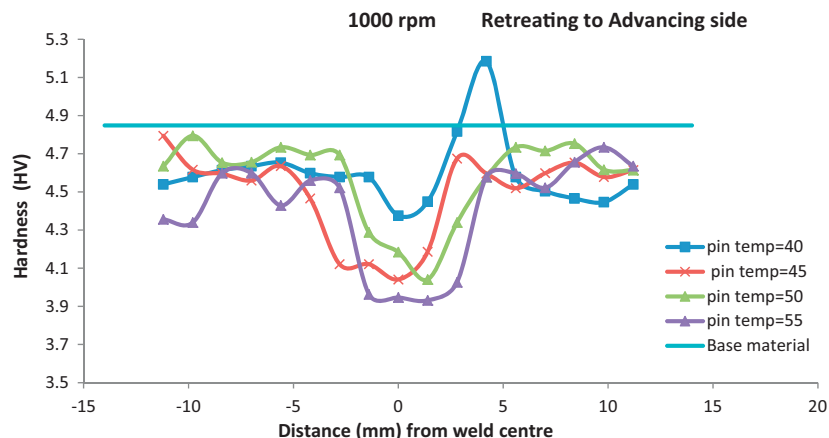
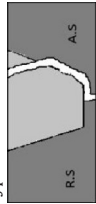


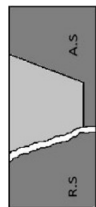
Fig. 17. Hardness plot at 1000 rpm and different tool-pin temperatures.

**Table 2**  
Joint efficiency, fracture type, and % elongation in friction-stir welded samples.

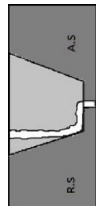
SNo.	RPM	Pin temperature (°C)	Ultimate tensile strength (Mpa)	Joint efficiency (%)	Types of fracture	Percentage elongation
1	1000	Room temperature	0.55	2.87	Type c	6.96
2	1000	40	8.17	41.01	Type c	6.56
3	1000	45	15.81	79.37	Type c	15.56
4	1000	50	15.36	77.11	Type c	15.08
5	1000	55	18.76	94.18	Type d	21.69
6	2000	Room temperature	4.5	23.62	Fractured at the root tip	1.37
7	2000	40	18.75	94.13	Type b	16.26
8	2000	45	20.78	104.32	Type a	20.17
9	2000	50	17.68	88.76	Type d	18.42
10	2000	55	19.66	98.69	Type c	18.05
11	3000	Room temperature	9.48	49.82	Type e	2.59
12	3000	40	17.9	89.86	Type e	14.29
13	3000	45	19.69	98.85	Type d	13.49
14	3000	50	15.72	78.92	Type d	20.7
15	3000	55	15.51	77.86	Type e	23.55



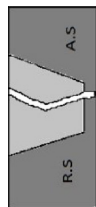
(a) Crack formed outside weld seam



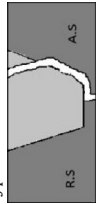
(b) Crack formed at the retreating interface



(c) Crack formed in the retreating side of weld seam



(d) Crack formed at the center of weld seam



(e) Crack formed in the advancing side of weld seam

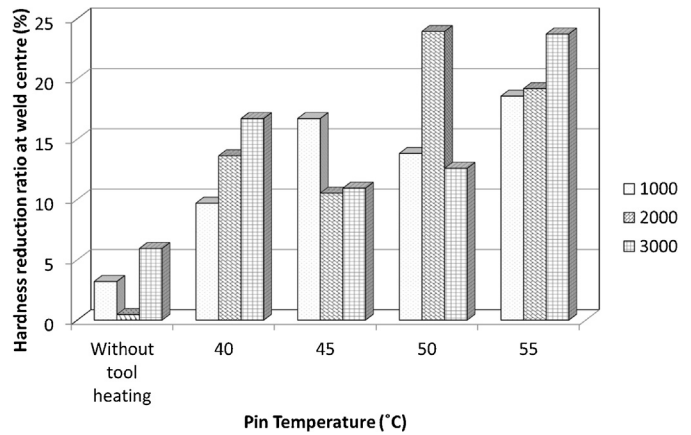


**Fig. 18.** Plot of hardness reduction ratio at weld center for different parameters.

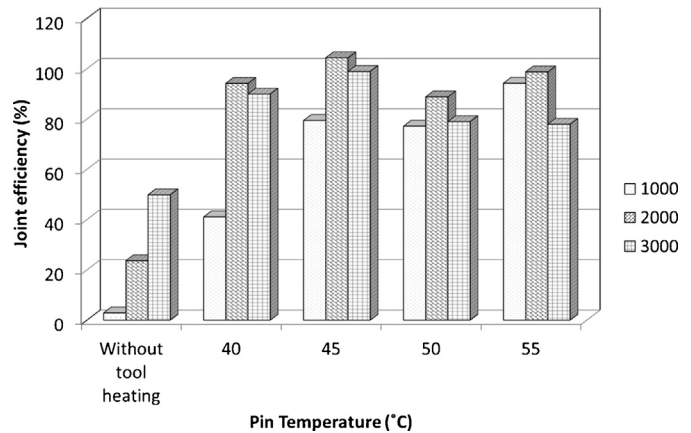


**Fig. 19.** Plot of joint efficiency for different parameters.

compared to the welds when tool was induction heated. Moreover, without tool heating, joint efficiency at 3000 rpm is higher indicating that frictional heat generated at higher rpm helps in good fusion between the seam and base material. Thus, when the tool is induction-heated, even at low rpm, little improvement in joint efficiency is obtained beyond 45 °C.

#### 4. Conclusion

A new technique of joining thermoplastic using friction-stir welding, namely i-FSW, is introduced wherein an induction-heated tool welds plates with a minimum amount of flash. The i-FSW technique is demonstrated through a case study on the welding of high-density polyethylene plates. Induction heating of tool enabled the plastic material to soften in a short time and to be easily stirred. As the tool-pin temperature increases, the hardness at the stir zone decreases due to the ductile nature of the joints. At high tool-pin temperatures the strength of the joint is governed by the ductile behavior of the material. Turbulence of the material, caused by the stirring action of the tool, was the main factor that governed the strength of the welds at low tool temperature. The optimum conditions for the maximum strength of the joints were a tool-pin temperature of 45 °C and a rotational speed of 2000 rpm. Microstructural examination revealed that, the strength of the friction-stir welded joint will be close to that of the base material if the overall width of the transition zone is small with less complex morphology. Such welds will also exhibit structural and chemical similarity with the base material and comparatively lesser reduction in hardness. The high strength values of joints

obtained by i-FSW could be attributed to good material mixing and the high level of crystallization in the weld seam, which are the main controls on mechanical strength. It is postulated that the effect of i-FSW on the crystallization mechanism could be an important factor, determining the mechanical performance of the joints, which merits further investigation in future studies.

## Acknowledgment

The authors acknowledge the support of Department of Science and Technology, Gov. of India for supporting the present investigation through grant Ref: SR/FTP/ETA-34/2009. The authors also acknowledge help provided by Dr. Prabusankar and Dr. Suhash Ranjan Dey of IIT Hyderabad in obtaining FTIR and DSC results.

## References

- [1] Nandan R, DebRoy T, Bhadeshia HKDH. Recent advances in friction-stir welding—process, weldment structure, and properties. *Prog Mater Sci* 2008;53(6):980–1023.
- [2] Thomes, W.M., Nicholas, E.D., Needham, J.C., Murch, M.G., Templesmith, P., Dawes, C.J., International Patent Application No.PCT/GB92/02203 and GB Patent Application No.9125978.8, USA, 1991.
- [3] Kumar K, Kailas SV. The role of friction stir welding tool on material flow and weld formation. *Mater Sci Eng* 2008;485:367–74.
- [4] Troughton M. Handbook of plastics joining. 2nd Ed Norwich: William Andrew Inc; 2008. p. 123–6.
- [5] Simões F, Rodrigues DM. Material flow and thermo–mechanical conditions during friction stir welding of polymers: literature review, experimental results, and empirical analysis. *Mater Design* 2014;59::344–51.
- [6] Strand S. Effects of friction stir welding on polymer microstructure. In: All Theses and Dissertations. Paper 42. 2004.
- [7] Jaiganesh V, Maruthu B, Gopinath E. Optimization of process parameters on friction stir welding of high density polypropylene plate. *Procedia Eng* 2014;97:1957–65.
- [8] Pirizadeh M, Azdast T, Ahmadi SR, Shishavan SM, Bagheri A. Friction stir welding of thermoplastics using a newly designed tool. *Mater Design* 2014;54:342–7.
- [9] Mendes N, Loureiro A, Martins C, Neto P, Pires JN. Morphology and strength of acrylonitrile butadiene styrene welds performed by robotic friction stir welding. *Mater Design* 2014;64:81–90.
- [10] Mendes N, Loureiro A, Martins C, Neto P, Pires JN. Effect of friction stir welding parameters on morphology and strength of Acrylonitrile Butadiene Styrene plate welds. *Mater Design* 2014;58:457–64.
- [11] Panneerselvam K, Lenin K. Joining of Nylon 6 plate by friction stir welding process using threaded pin profile. *Mater Design* 2014;53:302–7.
- [12] Hoseinlghab S, Mirjavadi SS, Sadeghian N, Jalili I, Azarbarmas M, Givi MKB. Influences of welding parameters on the quality and creep properties of friction stir welded polyethylene plates. *Mater Design* 2015;67:369–78.
- [13] Azarsa E, Mostafapour A. Experimental investigation on flexural behavior of friction stir welded high density polyethylene sheets. *J Manuf Process* 2014;16:149–55.
- [14] Bagheri A, Azdast T, Doniavi A. An experimental study on mechanical properties of friction stir welded ABS sheets. *Mater Design* 2013;43:402–9.
- [15] Sadeghian N, Givi MKB. Experimental optimization of the mechanical properties of friction-stir welded Acrylonitrile Butadiene Styrene sheets. *Mater Design* 2015;67:145–53.
- [16] Saeedy S, Givi MKB. Investigation of the effects of critical process parameters of friction stir welding of polyethylene. *J Eng Manuf* 2011;225:1305–10.
- [17] Arici A, Sinmaz T. Effects of double passes of the tool on friction stir welding of polyethylene. *J Mater Sci* 2005;40:3313–6.
- [18] Mostafapour A, Azarsa E. A study on the role of processing parameters in joining polyethylene sheets via heat assisted friction stir welding: investigating microstructure, tensile, and flexural properties. *Int J Phys Sci* 2012;7:647–54.
- [19] Arici A, Selale S. Effects of tool tilt angle on tensile strength and fracture locations of friction stir welding of polyethylene. *Sci Technol Weld Joi* 2007;12:536–9.
- [20] Kiss Z, Czigan T. Microscopic analysis of the morphology of seams in friction stir welded polypropylene. *Express Polym Lett* 2012;6:54–62.
- [21] Arbegast WJ. A flow-partitioned deformation zone model for defect formation during friction stir welding. *Scr Mater* 2008;58:372–6.
- [22] Inaniwa S, Kurabe Y, Miyashita Y, Hori H. Applicability of friction stir welding for several plastic materials. In: Fujii H, editor. Proceedings of 1<sup>st</sup> international joint symposium on joining and welding. Japan: Osaka; 2013. p. 137–42.